

Monitoring multimode processes: a modified PCA algorithm with continual learning ability

Jingxin Zhang, Donghua Zhou, *Fellow, IEEE*, and Maoyin Chen, *Member, IEEE*

Abstract—For multimode processes, one has to establish local monitoring models corresponding to local modes. However, the significant features of previous modes may be catastrophically forgotten when a monitoring model for the current mode is built. It would result in an abrupt performance decrease. Is it possible to make local monitoring model remember the features of previous modes? Choosing the principal component analysis (PCA) as a basic monitoring model, we try to resolve this problem. A modified PCA algorithm is built with continual learning ability for monitoring multimode processes, which adopts elastic weight consolidation (EWC) to overcome catastrophic forgetting of PCA for successive modes. It is called PCA-EWC, where the significant features of previous modes are preserved when a PCA model is established for the current mode. The computational complexity and key parameters are discussed to further understand the relationship between PCA and the proposed algorithm. Numerical case study and a practical industrial system in China are employed to illustrate the effectiveness of the proposed algorithm.

Note to Practitioners—Multimode process monitoring is increasingly significant as industrial systems generally operate in varying working conditions. However, most researches focus on multiple monitoring models for complex multimode processes and one local model fails to detect the fault accurately. When new modes come, the traditional multimode monitoring models need to be retrained from scratch, which is not suitable for industrial applications. This paper proposes a modified principal component analysis (PCA) with continual learning ability, where elastic weight consolidation is utilized to preserve the significant information of previous modes. Thus, one monitoring model can provide excellent performance for modes similar to previous ones. Besides, the proposed method is just a little complicated than traditional PCA and efficient for online monitoring. For practical industrial systems, such as large-scale power plants and chemical systems, the proposed method has outstanding ability to monitor various working conditions. In future, we will investigate the monitoring method with continual learning ability for multimode nonstationary processes.

Index Terms—Continual learning, multimode process monitoring, elastic weight consolidation, catastrophic forgetting

This work was supported by National Natural Science Foundation of China [grant numbers 62033008, 61751307, 61873143]. (Corresponding authors: Donghua Zhou; Maoyin Chen)

Jingxin Zhang is with the Department of Automation, Tsinghua University, Beijing 100084, China (e-mail: zjx18@mails.tsinghua.edu.cn).

Donghua Zhou is with College of Electrical Engineering and Automation, Shandong University of Science and Technology, Qingdao 266000, China and also with the Department of Automation, Tsinghua University, Beijing 100084, China (e-mail: zdh@mail.tsinghua.edu.cn).

Maoyin Chen is with the Department of Automation, Tsinghua University, Beijing 100001, China and also with School of Automation and Electrical Engineering, Linyi University, Linyi 276005, China (e-mail: mychen@tsinghua.edu.cn).

This work has been submitted to the IEEE Transactions on Automation Science and Engineering for possible publication. Copyright may be transferred without notice, after which this version may no longer be accessible.

I. INTRODUCTION

Process monitoring is increasingly important owing to the strict requirements for reliability and safety [1]–[4] and has received remarkable success with the development of data mining techniques [5]–[7]. However, traditional monitoring tasks require that the process has one operating mode and data follow the unimodal distribution [4]–[7]. However, in modern industrial systems, operating condition often changes with raw materials, product specifications, maintenance, etc [8]–[10]. The data generated from different modes are independent of each other and typically have different characteristics, such as mean, covariance and distribution [11], [12]. Thus, building an effective monitoring model for multimode processes is a challenging problem [13], [14].

Here current research status for monitoring multimode processes is reviewed briefly. Ma *et al.* [15] utilized local neighborhood standardization strategy to transfer the multimode data into unimodal distribution approximately and only one model was constructed for process monitoring without process knowledge. The multimode data were transformed to probability density by local probability density estimation that obeyed unimodal distribution, and then kernel principal component analysis (PCA) was performed to detect faults [16]. However, the transformation function is difficult to be determined accurately for complex systems. Recursive methods are regarded as a single-model based method and can update the parameters when the modes change [17], which are appropriate for slow switching of working conditions. Wang *et al.* [18] utilized Dirichlet process Gaussian mixed model to identify the mode automatically and then support vector data description was designed for each mode. In [19], PCA mixture models was proposed to reduce the dimension and the number of mixture components was optimized automatically by Bayesian Ying-Yang algorithm. The performance of mixture models are greatly influenced by the accuracy of mode identification and data from all potential modes are required before training. These approaches for monitoring multimode processes are generally sorted into two categories: 1) single models appropriate for every mode, where the multimodality features are removed by a transformation function and the monitoring model is built by the decision function in most cases [15], [16]; 2) multiple models where the mode is identified first and then local models are established in each mode [18]–[21]. In [22], methods for multimode processes were summarized and it revealed that most researches were relevant to multiple models.

For current multimode monitoring methods, they generally

require that training data must include all the modes. When two or more modes come sequentially, single model methods would train the model from scratch to acquire the transformation function based on data from all previous modes. However, it is intractable to obtain the appropriate transformation function especially for modern complicated systems with various modes. With regard to multiple models, local monitoring models are established corresponding to local modes. The important features of previous modes may be overwritten by new data when a single monitoring model is established for the current mode, thus delivering an abrupt decrease of performance if a single local monitoring model is used for multimode processes. Consequently, we need to retrain the monitoring models using all the data corresponding to all the modes from scratch. However, it consumes huge storage space and computing resources. State-of-the-art methods generally extract critical features from collected data, which are sufficient to reflect the data characteristics. And then the monitoring indexes are designed. Therefore, instead of storing original sensing data, is it possible to make local monitoring model remember the features of previous modes? Thus, a single model can show excellent performance for simultaneously monitoring the current mode and the future mode similar to previous modes. For example, two successive modes \mathcal{M}_1 and \mathcal{M}_2 need to be learned sequentially. If we build one model for the mode \mathcal{M}_2 based on the learned knowledge from the mode \mathcal{M}_1 , the single model would preserve the features for both modes with a small loss and provide outstanding performance for multimode processes. Once the mode \mathcal{M}_1 revisits, the single model can achieve acceptable monitoring results.

In the field of artificial intelligence, continual learning is exactly the technique that trains the new model based on the new mode data and the partial information about previous modes [23]–[25]. However, continual learning remains a long-standing challenge owing to “catastrophic forgetting” issue, namely, training a new model with new data would severely influence the performance of previous modes [26], [27]. Motivated by synaptic consolidation, Kirkpatrick *et al.* proposed elastic weight consolidation (EWC) to overcome catastrophic forgetting issue [28], which can learn consecutive tasks without forgetting previous tasks disastrously.

In this paper, we adopt the technique of EWC to overcome the catastrophic forgetting issue of PCA for multimode processes, referred to as PCA-EWC, where the significant features of previous modes are preserved if a PCA model is built for the current mode. An appropriate objective function is chosen to achieve continual learning, and the global optimal solution can be calculated by difference of convex functions (DC) [29]. The proposed PCA-EWC algorithm requires that similarity exists among different modes and it is easy to satisfy in practical applications because data in physical and chemical processes are generally governed by specific laws. The contributions of this paper are summarized as follows:

- (a) It provides a novel framework PCA-EWC for monitoring multimode processes. The major merit is that significant features of previous modes are preserved when a PCA model is designed for the current mode;
- (b) Different from single model based methods, PCA-EWC

updates the model using the learned knowledge without learning transformation function, which is appropriate for complex industrial systems;

- (c) Compared with multiple models, PCA-EWC preserves significant features from previous modes, and establishes a single model with continual learning ability that is effective for multiple modes simultaneously.

Here we discuss self-starting control chart (SSCC) and PCA-EWC for monitoring. SSCC calculates parameters and monitor the processes simultaneously [30], [31], where the parameters are updated based on the new collected data. Compared with statistical process monitoring, SSCC is often employed to monitor the start-up processes and short-run processes [32], [33], where data are not enough to establish the Hotelling’s T^2 chart. The proposed method is applied to multimode stationary processes, where abundant historical data have been stored or can be collected in a short time. This paper mainly aims at the stationary processes under different operating conditions. Furthermore, compared with PCA-EWC, SSCC forgets the significant information of previous modes and fails to monitor the similar modes without retraining.

The remaining parts are organized below. Section II reviews the EWC algorithm and reformulates PCA from the probabilistic perspective briefly, which lays the solid foundation of the proposed algorithm. Section III introduces PCA-EWC, the global optimal solution by DC programming, and the procedure for monitoring multimode processes. PCA-EWC is extended to more general multimode process monitoring and the specific procedure is presented in Section IV. Moreover, the relationship between PCA-EWC and PCA is discussed and the computational complexity is analyzed. A numerical case study and a practical plant subsystem are adopted to illustrate the effectiveness of the proposed algorithm in Section V. The concluding remark is given in Section VI.

II. PRELIMINARY

In this section, we introduce the core of EWC algorithm briefly, revisit the basic theory of PCA from the probabilistic perspective and it lays the solid foundation of PCA-EWC. Detailed information about EWC can be found in [28]. For convenience, we consider the successive monitoring tasks in successive modes \mathcal{M}_1 and \mathcal{M}_2 .

A. The revisit of EWC

EWC algorithm is an efficient method to overcome catastrophic forgetting issue [28]. It slows down the change on certain parameters based on the importance of previous tasks. For a learning method, learning a monitoring task principally adjusts the parameter θ by optimizing performance. Different configurations of θ may lead to the same result [34]. This makes it possible that parameter of the latter mode \mathcal{M}_2 , $\theta_{\mathcal{M}_2}^*$, is close to the parameter of previous mode \mathcal{M}_1 , $\theta_{\mathcal{M}_1}^*$. Thus, when building the monitoring model for mode \mathcal{M}_2 , partial information of mode \mathcal{M}_1 should be preserved, and $\theta_{\mathcal{M}_1}^*$ and $\theta_{\mathcal{M}_2}^*$ have a certain degree of similarity.

It is universally known that the learning processes are reformulated from the probabilistic perspective as follows.

It is transformed into finding the most probable parameter given data set \mathbf{X} . According to Bayesian rule, the conditional probability is calculated by prior probability $p(\theta)$ and data probability $p(\mathbf{X}|\theta)$:

$$\log p(\theta|\mathbf{X}) = \log p(\mathbf{X}|\theta) + \log p(\theta) - \log p(\mathbf{X}) \quad (1)$$

Suppose that data \mathbf{X} come from two independent modes, namely, mode \mathcal{M}_1 (\mathbf{X}_1) and mode \mathcal{M}_2 (\mathbf{X}_2). Then, (1) can be reformulated as:

$$\log p(\theta|\mathbf{X}) = \log p(\mathbf{X}_2|\theta) + \log p(\theta|\mathbf{X}_1) - \log p(\mathbf{X}) \quad (2)$$

Note that $\log p(\theta|\mathbf{X})$ denotes the posterior probability of the parameters given the entire dataset. $-\log p(\mathbf{X}_2|\theta)$ represents the loss function for mode \mathcal{M}_2 . Posterior distribution $\log p(\theta|\mathbf{X}_1)$ can reflect all information of mode \mathcal{M}_1 and significant information of mode \mathcal{M}_1 is contained in the posterior probability. The true posterior probability $p(\theta|\mathbf{X}_1)$ is generally intractable to compute and approximated by Laplace approximation in this paper [35], [36]. Detailed procedure has been presented in Appendix A.

According to Appendix A, the problem (2) is transformed to (39). However, the sample size N_1 has significant influence on quality of approximation [36]. A hyper-parameter $\lambda_{\mathcal{M}_1}$ is introduced to control the approximation better [36], and then the purpose of EWC is to minimize

$$\begin{aligned} -\log p(\theta|\mathbf{X}) \approx & -\log p(\mathbf{X}_2|\theta) + \frac{1}{2}(\theta - \theta_{\mathcal{M}_1}^*)^T \\ & (\lambda_{\mathcal{M}_1} \mathbf{F}_{\mathcal{M}_1} + \lambda_{prior} \mathbf{I})(\theta - \theta_{\mathcal{M}_1}^*) \end{aligned} \quad (3)$$

Let

$$\Omega_{\mathcal{M}_1} = \frac{1}{2}(\lambda_{\mathcal{M}_1} \mathbf{F}_{\mathcal{M}_1} + \lambda_{prior} \mathbf{I}) \quad (4)$$

The objective (3) is simplified by

$$\mathcal{J}(\theta) = \mathcal{J}_2(\theta, \mathbf{X}_2) + \mathcal{J}_{loss}(\theta, \theta_{\mathcal{M}_1}^*, \Omega_{\mathcal{M}_1}) \quad (5)$$

where $\mathcal{J}_2(\theta, \mathbf{X}_2) = -\log p(\mathbf{X}_2|\theta)$ represents the loss function of data \mathbf{X}_2 . $\mathcal{J}_{loss} = (\theta - \theta_{\mathcal{M}_1}^*)^T \Omega_{\mathcal{M}_1} (\theta - \theta_{\mathcal{M}_1}^*)$ is the quadratic penalty and measures the disparity between the last mode and the current mode. Note that we discard \mathbf{X}_1 after learning the model for mode \mathcal{M}_1 . The recent model (5) is built based on the current data \mathbf{X}_2 and the parameters from the last mode \mathcal{M}_1 , without the requirement of data \mathbf{X}_1 .

B. Probabilistic perspective of PCA

The observation data $\mathbf{x} \in R^m$ are generated from latent variables $\mathbf{y} \in R^l$ with $\mathbf{y} \sim N(\mathbf{0}, \mathbf{I})$, then

$$\mathbf{x} = \mathbf{P}\mathbf{y} + \boldsymbol{\mu} + \boldsymbol{\xi} \quad (6)$$

where $\boldsymbol{\mu} \in R^m$ is the mean value, noise $\boldsymbol{\xi}_i \sim N(0, \sigma^2)$, $i = 1, \dots, m$, σ^2 is constant but unknown, $\mathbf{P} \in R^{m \times l}$ is the loading matrix. Thus,

$$p(\mathbf{x}|\mathbf{y}, \mathbf{P}) = (2\pi\sigma^2)^{-\frac{m}{2}} \exp \left\{ -\frac{1}{2\sigma^2} \|\mathbf{x} - \mathbf{P}\mathbf{y} - \boldsymbol{\mu}\|^2 \right\} \quad (7)$$

A Gaussian prior probability over \mathbf{y} can be defined by

$$p(\mathbf{y}) = (2\pi)^{-\frac{l}{2}} \exp \left\{ -\frac{1}{2} \mathbf{y}^T \mathbf{y} \right\} \quad (8)$$

A Gaussian prior probability over \mathbf{P} is defined by

$$p(\mathbf{P}) = (2\pi)^{-\frac{ml}{2}} \exp \left\{ -\frac{1}{2} \text{tr}(\mathbf{P}^T \mathbf{P}) \right\} \quad (9)$$

Based on Bayesian theory, the posterior probability is calculated:

$$p(\mathbf{y}, \mathbf{P}|\mathbf{x}) = \frac{p(\mathbf{x}|\mathbf{y}, \mathbf{P})p(\mathbf{y})p(\mathbf{P})}{P(\mathbf{x})} \quad (10)$$

where

$$p(\mathbf{x}) = \int p(\mathbf{x}|\mathbf{y}, \mathbf{P})p(\mathbf{y})p(\mathbf{P})d\mathbf{y}d\mathbf{P}$$

which is constant with respect to \mathbf{y} and \mathbf{P} .

C. The foundation of PCA-EWC

PCA and EWC are reviewed from the probabilistic view. Then, the problem is to acquire the specific reformulation of (5) based on PCA. Thus, we need to calculate each term of right-hand side.

Based on (7), the objective of PCA is to minimize

$$\begin{aligned} & -\log p(\mathbf{X}|\mathbf{Y}, \mathbf{P}) \\ &= \sum_{n=1}^N -\ln p(\mathbf{x}_n|\mathbf{y}_n, \mathbf{P}) \\ &= \frac{N}{2} \{ m \ln(2\pi\sigma^2) + \frac{1}{\sigma^2} \text{tr}(\bar{\mathbf{X}}^T \bar{\mathbf{X}}) \} \end{aligned} \quad (11)$$

where $\bar{\mathbf{X}} = \mathbf{X} - \mathbf{1}\boldsymbol{\mu} - \mathbf{Y}\mathbf{P}^T$, $\mathbf{Y} = [\mathbf{y}_1, \dots, \mathbf{y}_N]$, $\mathbf{1}$ is the vector of all ones with appropriate dimension, N is the number of samples.

According to (6), we can get $\mathbf{Y} = \mathbf{X}\mathbf{P} - \mathbf{1}\boldsymbol{\mu}\mathbf{P} - \boldsymbol{\Xi}$, $\boldsymbol{\Xi}$ is the noise. Thus, $\bar{\mathbf{X}} = (\mathbf{X} - \mathbf{1}\boldsymbol{\mu})(\mathbf{I} - \mathbf{P}\mathbf{P}^T) - \boldsymbol{\Xi}\mathbf{P}$. The optimization of (11) is equivalent to minimizing

$$\begin{aligned} & \text{tr}(\bar{\mathbf{X}}^T \bar{\mathbf{X}}) \\ &= \text{tr}((\mathbf{I} - \mathbf{P}\mathbf{P}^T)(\mathbf{X} - \mathbf{1}\boldsymbol{\mu})^T(\mathbf{X} - \mathbf{1}\boldsymbol{\mu})(\mathbf{I} - \mathbf{P}\mathbf{P}^T)) \\ & \quad - 2\text{tr}((\mathbf{I} - \mathbf{P}\mathbf{P}^T)(\mathbf{X} - \mathbf{1}\boldsymbol{\mu})^T \boldsymbol{\Xi}\mathbf{P}) + \text{tr}(\mathbf{P}^T \boldsymbol{\Xi}^T \boldsymbol{\Xi}\mathbf{P}) \\ &= \text{tr}((\mathbf{I} - \mathbf{P}\mathbf{P}^T)(\mathbf{X} - \mathbf{1}\boldsymbol{\mu})^T(\mathbf{X} - \mathbf{1}\boldsymbol{\mu})) + N\sigma^2 \end{aligned} \quad (12)$$

with the constraint $\mathbf{P}^T \mathbf{P} = \mathbf{I}$.

Based on (11-12), the first term of (5) is designed as

$$\mathcal{J}_2(\mathbf{P}, \mathbf{X}) = \text{tr}((\mathbf{I} - \mathbf{P}\mathbf{P}^T)(\mathbf{X} - \mathbf{1}\boldsymbol{\mu})^T(\mathbf{X} - \mathbf{1}\boldsymbol{\mu})) \quad (13)$$

For the second term \mathcal{J}_{loss} , the key is to determine $\Omega_{\mathcal{M}_1}$, which is actually the second deviation of $-\log p(\mathbf{y}, \mathbf{P}|\mathbf{x})$ in (10). Therefore, the detailed form of (5) is acquired.

III. PCA-EWC PROCEDURE FOR MONITORING MULTIMODE PROCESSES

In this section, we present the procedure of PCA-EWC algorithm with continual learning ability and use DC programming to obtain the global optimal solution, which is then applied to monitor multimode processes. Here, we consider monitoring tasks for two successive modes \mathcal{M}_1 and \mathcal{M}_2 .

A. PCA-EWC algorithm

Assume that there exist two sequential monitoring tasks corresponding to two successive modes \mathcal{M}_1 and \mathcal{M}_2 . In addition,

the basic PCA is used to build a monitoring model. The normal data are collected as $\mathbf{X}_1 \in R^{N_1 \times m}$, $\mathbf{X}_2 \in R^{N_2 \times m}$, where N_1 and N_2 are the number of samples, and m is the number of variables. For convenient description, the data are already scaled to zero mean and unit variance, namely, $\mu = \mathbf{0}$.

With regard to the monitoring task for the mode \mathcal{M}_1 , the projection matrix is $\mathbf{P}_{\mathcal{M}_1} \in R^{m \times l}$ through PCA and l is the number of principal components determined by cumulative percent variance approach. Thus, the purpose is to find a proper projection matrix \mathbf{P} , which is effective to monitor modes \mathcal{M}_1 and \mathcal{M}_2 simultaneously.

As illustrated in Fig. 1, after the first monitoring task in the mode \mathcal{M}_1 is learned by PCA, the parameter is at $\mathbf{P}_{\mathcal{M}_1}$ (the black arrow). If we train the monitoring task for the mode \mathcal{M}_2 alone (the green arrow), the learned knowledge from the mode \mathcal{M}_1 would be destroyed or even completely overwritten by new data in the worst case. EWC enables us to monitor the mode \mathcal{M}_2 without suffering important loss on the mode \mathcal{M}_1 (the red arrow), by preserving the partial information for the mode \mathcal{M}_1 .

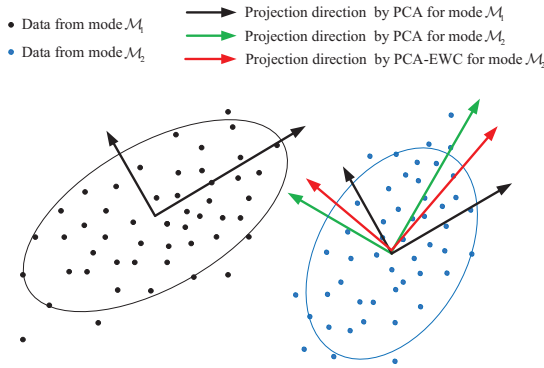


Fig. 1. Geometric illustration of EWC-PCA

For simplicity, we assume that the number of principal components remains the same for two successive modes. According to (5), the objective function is described as:

$$\mathcal{J}(\mathbf{P}) = \mathcal{J}_2(\mathbf{P}) + \mathcal{J}_{loss}(\mathbf{P}, \mathbf{P}_{\mathcal{M}_1}, \Omega_{\mathcal{M}_1}) \quad (14)$$

where $\mathcal{J}_2(\mathbf{P})$ is the loss function for monitoring task in the mode \mathcal{M}_2 only, $\mathcal{J}_{loss}(\mathbf{P}, \mathbf{P}_{\mathcal{M}_1}, \Omega_{\mathcal{M}_1})$ represents the loss function of previous mode \mathcal{M}_1 , and $\Omega_{\mathcal{M}_1}$ is positive definite and calculated by (4).

For PCA, maximizing the posterior probability is transformed to (13), thus $\mathcal{J}_2(\mathbf{P})$ is reformulated as

$$\mathcal{J}_2(\mathbf{P}) = \text{tr}(\mathbf{X}_2^T \mathbf{X}_2) - \text{tr}(\mathbf{P}^T \mathbf{X}_2^T \mathbf{X}_2 \mathbf{P}) \quad (15)$$

where the constraint $\mathbf{P}^T \mathbf{P} = \mathbf{I}$ with $\mathbf{P} \in R^{m \times l}$, $\mu = \mathbf{0}$.

According to (3-5), $\mathcal{J}_{loss}(\mathbf{P}, \mathbf{P}_{\mathcal{M}_1}, \Omega_{\mathcal{M}_1})$ is expressed by:

$$\begin{aligned} & \mathcal{J}_{loss}(\mathbf{P}, \mathbf{P}_{\mathcal{M}_1}, \Omega_{\mathcal{M}_1}) \\ &= \text{tr}\{(\mathbf{P} - \mathbf{P}_{\mathcal{M}_1})^T \Omega_{\mathcal{M}_1} (\mathbf{P} - \mathbf{P}_{\mathcal{M}_1})\} \\ &= \text{tr}(\mathbf{P}^T \Omega_{\mathcal{M}_1} \mathbf{P}) - 2\text{tr}(\mathbf{P}^T \Omega_{\mathcal{M}_1} \mathbf{P}_{\mathcal{M}_1}) + \text{tr}(\mathbf{P}_{\mathcal{M}_1}^T \Omega_{\mathcal{M}_1} \mathbf{P}_{\mathcal{M}_1}) \\ &= \|\mathbf{P} - \mathbf{P}_{\mathcal{M}_1}\|_{\Omega_{\mathcal{M}_1}}^2 \end{aligned} \quad (16)$$

Algorithm 1 PCA-EWC using DC programming.

Input: parameter ϵ

Output: \mathbf{P}_{k+1} , that yields the minimum of $\mathcal{J}(\mathbf{P}) = G(\mathbf{P}) - H(\mathbf{P})$ with constraint $\mathbf{P}^T \mathbf{P} = \mathbf{I}$

- 1: Let $\mathbf{P}_0 = \mathbf{P}_{\mathcal{M}_1}$ be an initial solution
- 2: Set the initial counter $k = 0$
- 3: Linearize the concave part by computing $\mathbf{U}_k \in \partial H(\mathbf{P}_k)$ and $\mathbf{U}_k = 2\mathbf{X}_2^T \mathbf{X}_2 \mathbf{P}_k$
- 4: Compute \mathbf{P}_{k+1} by solving the problem (23), and $\mathbf{P}_{k+1} = \mathbf{W}_k \mathbf{I}_{m,l} \mathbf{V}_k^T$
- 5: Let $k = k + 1$
- 6: Go to step 3 until $\|\mathbf{P}_{k+1} - \mathbf{P}_k\|_F^2 < \epsilon$

Obviously, $\mathcal{J}_{loss}(\mathbf{P}, \mathbf{P}_{\mathcal{M}_1}, \Omega_{\mathcal{M}_1})$ measures the difference of current parameter $\mathbf{P}_{\mathcal{M}_1}$ and the optimal parameter \mathbf{P} .

Substituting (15-16) into (14), we can get

$$\begin{aligned} & \mathcal{J}(\mathbf{P}) \\ &= \text{tr}(\mathbf{P}^T \Omega_{\mathcal{M}_1} \mathbf{P}) - \text{tr}(\mathbf{P}^T \mathbf{X}_2^T \mathbf{X}_2 \mathbf{P}) - 2\text{tr}(\mathbf{P}^T \Omega_{\mathcal{M}_1} \mathbf{P}_{\mathcal{M}_1}) \\ & \quad + \underbrace{\{\text{tr}(\mathbf{X}_2^T \mathbf{X}_2) + \text{tr}(\mathbf{P}_{\mathcal{M}_1}^T \Omega_{\mathcal{M}_1} \mathbf{P}_{\mathcal{M}_1})\}}_{\text{constant}} \end{aligned} \quad (17)$$

Problem (17) is nonconvex and intractable to acquire the global optimal solution by stochastic gradient descent method. Let $G(\mathbf{P}) = \text{tr}(\mathbf{P}^T \Omega_{\mathcal{M}_1} \mathbf{P}) - 2\text{tr}(\mathbf{P}^T \Omega_{\mathcal{M}_1} \mathbf{P}_{\mathcal{M}_1})$, $H(\mathbf{P}) = \text{tr}(\mathbf{P}^T \mathbf{X}_2^T \mathbf{X}_2 \mathbf{P})$. Thus, $\mathcal{J}(\mathbf{P}) = G(\mathbf{P}) - H(\mathbf{P}) + \text{constant}$. The original problem (14) can be transformed into

$$\begin{aligned} \min_{\mathbf{P}} \quad & \mathcal{J}(\mathbf{P}) \iff \min_{\mathbf{P}} \quad G(\mathbf{P}) - H(\mathbf{P}) \\ \text{s.t.} \quad & \mathbf{P}^T \mathbf{P} = \mathbf{I} \in R^{l \times l} \end{aligned} \quad (18)$$

As $G(\mathbf{P})$ and $H(\mathbf{P})$ are obviously convex, the objective function (18) is formulated as DC programming problem [37].

B. Global optimal solution based on DC programming

Inspired by solution in [38], we adopt DC programming to optimize (18), as summarized in Algorithm 1. The procedure includes linearizing the concave part and solving the convex subproblem part.

1) *Linearizing the concave part:* Assume that \mathbf{P}_k is the solution at k th iteration in Algorithm 1. The linearization of the second component $H(\mathbf{P})$ is given by

$$H_l(\mathbf{P}) = H(\mathbf{P}_k) + \langle \mathbf{P} - \mathbf{P}_k, \mathbf{U}_k \rangle, \mathbf{U}_k \in \partial H(\mathbf{P}_k) \quad (19)$$

Then, (18) can be approximated by solving a convex program since $H_l(\mathbf{P})$ is a linear function of \mathbf{P} . In order to approximate the concave part, we need to compute the subgradient \mathbf{U}_k . Since $\mathbf{U} \in \frac{\partial H(\mathbf{P})}{\partial \mathbf{P}} = 2\mathbf{X}_2^T \mathbf{X}_2 \mathbf{P}$, let $\mathbf{U}_k = 2\mathbf{X}_2^T \mathbf{X}_2 \mathbf{P}_k$.

2) *Solving the convex subproblem:* After obtaining a subgradient \mathbf{U}_k of $H(\mathbf{P})$ at \mathbf{P}_k , we can replace $H(\mathbf{P})$ by its linearization. Therefore, (18) is approximated by the following convex semidefinite programming

$$\mathbf{P}_{k+1} \doteq \arg \min_{\mathbf{P}^T \mathbf{P} = \mathbf{I}} G(\mathbf{P}) - \langle \mathbf{P}, \mathbf{U}_k \rangle \quad (20)$$

TABLE I
SIMULATION SCHEME OF PCA-EWC

	Training resources	Training model label	Algorithm	Testing data
Situation 1	Training data 1	Model A	PCA	Testing data 1
Situation 2	Training data 2 + Model A	Model B	PCA-EWC	Testing data 2
Situation 3	-	Model B	-	Testing data 3
Situation 4	Training data 2	Model C	PCA	Testing data 3

Since $\Omega_{\mathcal{M}_1}$ is positive definite, let $\Omega_{\mathcal{M}_1} = \mathbf{L}^T \mathbf{L}$ and \mathbf{L} is the triangle matrix. Thus, we can get

$$\begin{aligned}
 G(\mathbf{P}) - & \langle \mathbf{P}, \mathbf{U}_k \rangle \\
 = & \text{tr}(\mathbf{P}^T \Omega_{\mathcal{M}_1} \mathbf{P}) - 2\text{tr}(\mathbf{P}^T \Omega_{\mathcal{M}_1} \mathbf{P}_{\mathcal{M}_1}) - 2\text{tr}(\mathbf{P}^T \mathbf{X}_2^T \mathbf{X}_2 \mathbf{P}) \\
 = & \langle \mathbf{L}\mathbf{P}, \mathbf{L}\mathbf{P} \rangle - 2\langle \mathbf{L}\mathbf{P}, \mathbf{L}\mathbf{P}_{\mathcal{M}_1} + (\mathbf{L}^T)^{-1} \mathbf{X}_2^T \mathbf{X}_2 \mathbf{P}_k \rangle \\
 = & \|\mathbf{Z}_k - \mathbf{L}\mathbf{P}\|_F^2 - \|\mathbf{Z}_k\|_F^2
 \end{aligned} \tag{21}$$

where $\mathbf{Z}_k = \mathbf{L}\mathbf{P}_{\mathcal{M}_1} + (\mathbf{L}^T)^{-1} \mathbf{X}_2^T \mathbf{X}_2 \mathbf{P}_k$, and it is constant at $k + 1$ th iteration.

Then, the optimization problem (20) is equivalent to

$$\mathbf{P}_{k+1} = \arg \min_{\mathbf{P}^T \mathbf{P} = \mathbf{I}} \|\mathbf{Z}_k - \mathbf{L}\mathbf{P}\|_F^2 \tag{22}$$

Motivated by section 3.5 in [39], (22) is reformulated as

$$\mathbf{P}_{k+1} = \arg \min_{\mathbf{P}^T \mathbf{P} = \mathbf{I}} \|\mathbf{P} - \mathbf{L}^T \mathbf{Z}_k\|_F^2 \tag{23}$$

Let $\mathbf{R}_k = \mathbf{L}^T \mathbf{Z}_k = \Omega_{\mathcal{M}_1} \mathbf{P}_{\mathcal{M}_1} + \mathbf{X}_2^T \mathbf{X}_2 \mathbf{P}_k$. According to the lemma in [39], we can obtain that $\mathbf{P}_{k+1} = \mathbf{W}_k \mathbf{I}_{m,l} \mathbf{V}_k^T$, where $\mathbf{W}_k \in R^{m \times m}$ and $\mathbf{V}_k \in R^{l \times l}$ are left and right singular vectors of the singular vector decomposition (SVD) of \mathbf{R}_k . Detailed derivation process can be found in [39]. Notice that the optimal projection matrix for the mode \mathcal{M}_2 is denoted as $\mathbf{P}_{\mathcal{M}_2}$ for convenience.

C. Summary

Similar to many machine learning methods, two test statistics are designed for process monitoring. Hotelling's T^2 is designed to monitor the principal component subspace and squared prediction error (SPE) is calculated for monitoring the residual component subspace.

$$T^2 = \mathbf{x} \mathbf{P} \left(\frac{\mathbf{P}^T \mathbf{X}^T \mathbf{X} \mathbf{P}}{N-1} \right)^{-1} \mathbf{P}^T \mathbf{x}^T \tag{24}$$

$$\text{SPE} = \mathbf{x} (\mathbf{I} - \mathbf{P} \mathbf{P}^T) \mathbf{x}^T \tag{25}$$

Note that $\mathbf{P} = \mathbf{P}_{\mathcal{M}_1}$, $\mathbf{X} = \mathbf{X}_1$ and $N = N_1$ for the mode \mathcal{M}_1 , $\mathbf{P} = \mathbf{P}_{\mathcal{M}_2}$, $\mathbf{X} = \mathbf{X}_2$ and $N = N_2$ for the mode \mathcal{M}_2 .

Given a confidence limit α , the thresholds of two statistics are calculated by kernel density estimation [40] and denoted as J_{th,T^2} and $J_{th,SPE}$. Note $\alpha = 0.99$ in this paper. Thus, the detection logic satisfies

$$T^2 \leq J_{th,T^2} \text{ and } \text{SPE} \leq J_{th,SPE} \Rightarrow \text{fault free, otherwise faulty.}$$

We strive to highlight the continual learning ability of PCA-EWC for monitoring multimode processes, and illustrate the memory characteristic of current model for previous modes or similar modes. We set four combinations of training data

and testing data to interpret the effectiveness of PCA-EWC, as depicted in Table I. We define that Data 1 from the mode \mathcal{M}_1 and Data 3 follow basically the same or similar distribution. Data 2 are originated from the mode \mathcal{M}_2 . Data 1, Data 2 and Data 3 are collected successively. For every Data i , $i = 1, 2, 3$, normal training data and the corresponding testing data are denoted as training data i and testing data i . Notice that Situations 1 and 2 must be learned sequentially. For convenience and intuitive understanding, we recur to the information in Table I to summarize the monitoring procedure.

The off-line modeling phase is depicted as follows.

- For Situation 1, calculate the mean and variance of training data 1 and normalize data;
- Train PCA model using training data 1 and calculate the projection matrix $\mathbf{P}_{\mathcal{M}_1}$. The training model is denoted as Model A;
- Calculate mean and variance of training data 2 and normalize data;
- Train the new mode \mathcal{M}_2 using PCA-EWC, and calculate the optimal projection matrix $\mathbf{P}_{\mathcal{M}_2}$ according to Algorithm 1. This training model is recorded as Model B;
- With regard to Situation 4, train the monitoring model for the mode \mathcal{M}_2 by PCA, labeled by Model C;
- For Situations 1, 2 and 4, calculate the test statistics by (24) and (25);
- Calculate the corresponding thresholds, namely, J_{th,T^2} and $J_{th,SPE}$.

The on-line monitoring phase is presented below.

- For Situation 1, preprocess the testing data 1 based on its mean and variance, and then utilize Model A to calculate two test statistics related to $\mathbf{P}_{\mathcal{M}_1}$ by (24) and (25);
- For Situation 2, preprocess the testing data 2 from mode \mathcal{M}_2 , and then employ Model B to calculate two test statistics relevant to $\mathbf{P}_{\mathcal{M}_2}$ by (24) and (25);
- With regard to Situation 3, preprocess the testing data 3 and adopt Model B to calculate the test statistics related to $\mathbf{P}_{\mathcal{M}_2}$ based on (24) and (25);
- For Situation 4, preprocess the testing data 3 from the mode \mathcal{M}_1 and apply Model C to calculate two test statistics;
- Defect faults according to the fault detection logic.

We assume that the process works under the normal condition at stable initial stage when a new operating mode appears. Thus, mean and variance are calculated by a few normal data of the new mode and then utilized to preprocess the corresponding testing data. Two indexes are adopted to evaluate the performance, namely, fault detection rate (FDR) and false alarm rate (FAR). The calculation method refers to

[40]. Furthermore, detection delay (DD) is valuable and the primary evaluation indicator for practical industrial systems. The detection delay refers to the number of samples that the fault is detected later than the abnormal time recorded.

Remark: Note that Model B is built by the significant features from the mode \mathcal{M}_1 and new data from the mode \mathcal{M}_2 . If the performance of Situation 3 is still excellent, the monitoring model based on PCA-EWC is regarded to have overcome catastrophic forgetting issue and partial information of previous modes is enough to provide favorable capability. When the performance of Situations 2 and 3 is similarly excellent, it is demonstrated that PCA-EWC is effective to monitor the current mode and the future mode similar to previous modes. Situation 4 is designed as a comparative study. If the monitoring effect of Situation 4 is poor, it is proved that traditional PCA suffers from catastrophic forgetting issue and fails to detect novelty for multimode processes. In one word, it is desired that the performance of Situations 1-3 is outstanding while the performance of Situation 4 is poor.

IV. MODEL EXTENSION AND DISCUSSION

The PCA-EWC for multimode process monitoring is extended to general cases in this section. Beside, more detailed information and performance are discussed.

A. Model Extension

We discuss three successive modes for process monitoring and give the more general procedure briefly.

When data \mathbf{X}_3 from mode \mathcal{M}_3 are collected, the Bayesian posterior decomposes below:

$$\log p(\theta|\mathbf{X}) = \log p(\mathbf{X}_3|\theta) + \log p(\theta|\mathbf{X}_1, \mathbf{X}_2) + \text{constant} \quad (26)$$

Here, \mathbf{X} contain data from three modes. After learning the model from mode \mathcal{M}_1 , data \mathbf{X}_1 are discarded. We adopt recursive Laplace approximation to approximate (26), as presented in Appendix B.

Similar to (5), the objective function is described as:

$$\mathcal{J}(\theta) = \mathcal{J}_3(\theta, \mathbf{X}_3) + \mathcal{J}_{\text{loss}}(\theta, \theta_{\mathcal{M}_2}^*, \Omega_{\mathcal{M}_2}) \quad (27)$$

Then, the above derivation is extended to more general cases. When a new mode \mathcal{M}_n appears and needs to be learned, let the data denote as \mathbf{X}_n . The objective is

$$\begin{aligned} \log p(\theta|\mathbf{X}) &= \log p(\mathbf{X}_n|\theta) + \log p(\theta|\mathbf{X}_1, \dots, \mathbf{X}_{n-1}) \\ &\quad + \text{constant} \end{aligned} \quad (28)$$

Based on recursive Laplace approximation in Appendix B, the posterior probability is approximated as:

$$\begin{aligned} \log p(\theta|\mathbf{X}) &\approx \log p(\mathbf{X}_n|\theta) - (\theta - \theta_{\mathcal{M}_{n-1}}^*)^T \\ &\quad \Omega_{\mathcal{M}_{n-1}}(\theta - \theta_{\mathcal{M}_{n-1}}^*) + \text{constant} \end{aligned} \quad (29)$$

where

$$\Omega_{\mathcal{M}_{n-1}} = \Omega_{\mathcal{M}_{n-2}} + \frac{1}{2}\lambda_{\mathcal{M}_{n-1}}\mathbf{F}_{\mathcal{M}_{n-1}}, n \geq 3 \quad (30)$$

$\mathbf{F}_{\mathcal{M}_{n-1}}$ is the Fisher information matrix of mode \mathcal{M}_{n-1} , $\lambda_{\mathcal{M}_{n-1}}$ is the hyper-parameter that can measure the importance of the mode. Then, the objective function is designed as

$$\mathcal{J}(\mathbf{P}) = \mathcal{J}_n(\mathbf{P}) + \mathcal{J}_{\text{loss}}(\mathbf{P}, \mathbf{P}_{\mathcal{M}_{n-1}}, \Omega_{\mathcal{M}_{n-1}}) \quad (31)$$

where $\mathbf{P}_{\mathcal{M}_{n-1}}$ is the optimal projection matrix based on PCA-EWC for the previous mode \mathcal{M}_{n-1} . $\mathcal{J}_n(\mathbf{P})$ is the loss function for the mode \mathcal{M}_n by PCA. Similarly,

$$\mathcal{J}_n(\mathbf{P}) = \text{tr}(\mathbf{X}_n^T \mathbf{X}_n) - \text{tr}(\mathbf{P}^T \mathbf{X}_n^T \mathbf{X}_n \mathbf{P}) \quad (32)$$

$$\mathcal{J}_{\text{loss}}(\mathbf{P}, \mathbf{P}_{\mathcal{M}_{n-1}}, \Omega_{\mathcal{M}_{n-1}}) = \|\mathbf{P} - \mathbf{P}_{\mathcal{M}_{n-1}}\|_{\Omega_{\mathcal{M}_{n-1}}}^2 \quad (33)$$

Hence,

$$\begin{aligned} \mathcal{J}(\mathbf{P}) &= \text{tr}(\mathbf{P}^T \Omega_{\mathcal{M}_{n-1}} \mathbf{P}) - 2\text{tr}(\mathbf{P}^T \Omega_{\mathcal{M}_{n-1}} \mathbf{P}_{\mathcal{M}_{n-1}}) \\ &\quad - \text{tr}(\mathbf{P}^T \mathbf{X}_n^T \mathbf{X}_n \mathbf{P}) \\ &\quad + \underbrace{\{\text{tr}(\mathbf{X}_n^T \mathbf{X}_n) + \text{tr}(\mathbf{P}_{\mathcal{M}_{n-1}}^T \Omega_{\mathcal{M}_{n-1}} \mathbf{P}_{\mathcal{M}_{n-1}})\}}_{\text{constant}} \end{aligned} \quad (34)$$

Minimization of (34) is settled by DC programming in Section III-B, denoted as $\mathbf{P}_{\mathcal{M}_n}$. The monitoring scheme can also be found in Section III-C.

B. Discussion

1) *The influence of parameter setting:* Here we discuss the influence of $\lambda_{\mathcal{M}_1}$ when learning the monitoring task from the mode \mathcal{M}_2 . The positive definite matrix Ω is computed based on Fisher information matrix of mode \mathcal{M}_1 and $\lambda_{\mathcal{M}_1}$. Large value of $\lambda_{\mathcal{M}_1}$ indicates that the previous mode would play a significant role and more information is expected to be retained. Generally, $\lambda_{\mathcal{M}_1}$ is determined by prior knowledge.

Two extreme cases are described to strength understanding. When $\lambda_{\mathcal{M}_1} = 0$, the information of previous mode \mathcal{M}_1 is completely forgotten. PCA-EWC is equivalent to standard PCA and the training parameter of the mode \mathcal{M}_2 is shown by the green arrow in Fig. 1. When $\lambda_{\mathcal{M}_1} \rightarrow \infty$, all information of previous mode is retained and the information from the current mode is nearly neglected. Thus, the training parameter of the mode \mathcal{M}_2 approximates to $\mathbf{P}_{\mathcal{M}_1}$ (the dark arrow in Fig. 1).

2) *Computational complexity analysis:* The computational complexity mainly contains training models of the mode \mathcal{M}_1 by PCA and the mode \mathcal{M}_2 by PCA-EWC. In Algorithm 1, the computation focuses on the SVD of $\mathbf{R}_k \in R^{m \times l}$. The term *flam* is utilized to measure the operation counts. The SVD of \mathbf{X}_1 needs $\frac{3}{2}m^2N_1 + \frac{9}{2}m^3$ flam. For the monitoring task from the mode \mathcal{M}_2 , the matrices $\Omega_{\mathcal{M}_1} \mathbf{P}_{\mathcal{M}_1} \in R^{m \times l}$ and $\mathbf{X}_2^T \mathbf{X}_2 \in R^{m \times m}$ are actually constant, which require $2m^2l$ flam and $2m^2N_2$ flam. Then, the optimal $\mathbf{P}_{\mathcal{M}_2}$ is acquired after t times iteration. The calculation of \mathbf{R}_k needs $2m^2l + ml$ flam and the SVD of \mathbf{R}_k requires $\frac{3}{2}l^2m + \frac{9}{2}l^3$ flam. The calculation of matrix $\mathbf{W}_k \mathbf{V}_k^T$ requires $2m^2l$ flam. Overall, the time complexity of Algorithm 1 is $(4m^2l + \frac{3}{2}l^2m + \frac{9}{2}l^3 + ml)t + 2m^2l + 2m^2N_2$ flam. PCA-EWC adds at most $(4m^2l + \frac{3}{2}l^2m + \frac{9}{2}l^3 + ml)t + 2m^2l$ flam compared with

PCA. In practical applications, the initial setting of Algorithm 1 makes it converge fast. In conclusion, PCA-EWC is a little complicated compared with PCA, especially for large data set.

3) *Potential limitation and solution*: This method requires the existence of similarity in different modes, thus the retained information about previous modes would be useful for new modes. This requirement is relatively easy to satisfy especially for industrial systems, because the systems follow similar physical or chemical laws for different operating modes. Obviously, the performance of PCA-EWC would be affected by similarity in operating modes. The performance may keep excellent if data from various modes are considerably similar. However, if data from new mode are completely different from the previous modes, this method can not deliver excellent performance. Aimed at this case, the monitoring model would be retrained or the transfer learning would be adopted if inner relationship between the new mode and the previous ones can be found. Briefly, this method is appropriate to monitor the modes, the data distribution of which is similar or even the identical to the previous ones.

V. EXPERIMENTAL STUDY

This section adopts a numerical case and a practical pulverizing system to illustrate the continual learning ability of PCA-EWC for monitoring multimode processes. Through different combinations of training data and testing data in Table I, the continual learning ability of PCA-EWC is illustrated. Besides, Gaussian mixture models (GMMs) and recursive PCA (RPCA) are adopted to compare with the proposed method. The simulation results illustrate that PCA-EWC delivers optimal performance for monitoring successive modes.

A. Numerical case study

We employ the following case [41]:

$$\begin{bmatrix} x_1 \\ x_2 \\ x_3 \\ x_4 \\ x_5 \\ x_6 \\ x_7 \\ x_8 \end{bmatrix} = \begin{bmatrix} 0.95 & 0.82 & 0.94 \\ 0.23 & 0.45 & 0.92 \\ -0.61 & 0.62 & 0.41 \\ 0.49 & 0.79 & 0.89 \\ 0.89 & -0.92 & 0.06 \\ 0.76 & 0.74 & 0.35 \\ 0.46 & 0.58 & 0.81 \\ -0.02 & 0.41 & 0.01 \end{bmatrix} \begin{bmatrix} s_1 \\ s_2 \\ s_3 \end{bmatrix} + e \quad (35)$$

where the noise $e \in R^8$ follows Gaussian distribution $e_i \sim N(0, 0.001)$, $i = 1, \dots, 8$. We generate four sequential data successively as follows:

- Data 1: $s_1 \sim U([-10, -9.7])$, $s_2 \sim N(-5, 1)$, and $s_3 \sim U([2, 3])$;
- Data 2: $s_1 \sim U([-6, -5.7])$, $s_2 \sim N(-1, 1)$, and $s_3 \sim U([3, 4])$;
- Data 3: $s_1 \sim U([-10, -9.7])$, $s_2 \sim N(-5, 1)$, and $s_3 \sim U([2, 3])$;
- Data 4: $s_1 \sim U([-9, -8.7])$, $s_2 \sim N(-5, 1)$, and $s_3 \sim U([3, 4])$.

where $U([-10, -9.7])$ represents the uniform distribution between -10 and -9.7 , and so on. Data 1 and 3 follow the

same distribution and come from the mode M_1 . Data 2 are collected from the mode M_2 . Obviously, Data 4 have a certain degree of similarity with Data 1 and 2, which can also be verified and measured by Wasserstein distance. Jarque-Bera hypothesis test is adopted to evaluate the Gaussianity of data. The test statistics are lower than critical value 5.9282. Thus, the data follow multivariate Gaussian distribution under the confidence level 95%.

1000 normal samples from Data 1 and 2 are generated to train the model, denoted as training data 1 and training data 2, respectively. 1000 samples from Data i , $i = 1, 2, 3, 4$, are collected for testing and the novelty scenarios are designed below:

- Fault 1: the variable x_3 is added by 0.2 from 501th sample;
- Fault 2: the variable x_6 is added by 0.2 from 501th sample;
- Fault 3: the slope drift occurs in the variable x_1 from 501th sample and the slope rate is 0.002.

Take Fault 1 for instance, the variable x_3 is added by 0.2 in Data i , $i = 1, 2, 3, 4$, which constitutes the testing data i . Four situations are designed to illustrate the effectiveness of PCA-EWC, as depicted in Table I. GMMs and RPCA are adopted to compare with the proposed method. Another five situations are designed below.

- Situation 5: the training model is Model B and the testing data comes from Data 4 to illustrate the effectiveness of PCA-EWC on similar mode;
- Situation 6: the GMMs-based monitoring model is built based on the normal data from Data 1 and Data 2, and the testing data are from Data 3 to illustrate the effectiveness on the previous trained mode;
- Situation 7: the training model is the same with Situation 6, and the testing data are from Data 4 to illustrate the effectiveness on similar mode;
- Situation 8: data contain the normal samples from Data 1 and Data 2, testing data from Data 3, which is employed to illustrate the effect of RPCA for the previous mode;
- Situation 9: data include the normal samples from Data 1 and Data 2, testing data from Data 4, which is employed to illustrate the effect of RPCA for monitoring the similar mode.

We conduct 1000 independent repeated experiments and the results are summarized in Table II. The indexes are shown in the form of ‘mean value/standard deviation’. FDR, FAR and DD are considered to evaluate the performance of the proposed PCA-EWC. The consequences of Fault 1 and Fault 2 are similar and stable. Besides, faults can be detected accurately and timely, except for Situation 4. For Fault 3, the FDRs of Situations 1-3 and 5 for Fault 3 are less than 100% because the abnormal amplitude at initial abnormal time is so small that can not be detected immediately. However, the detection effect of Situation 4 is still poor when the abnormal amplitude increases. For Situations 6-9, the FARs are pretty high and even approach to 100%, which indicate that GMMs and RPCA fail to monitor the same or similar modes.

Then, we select one independent experiment to explain the performance specifically. According to Table II, the simulation results of Fault 1 and Fault 2 are analogous. We just choose Fault 1 as a representative. For every fault, the results of Situation 1 are stable and excellent, which are employed to

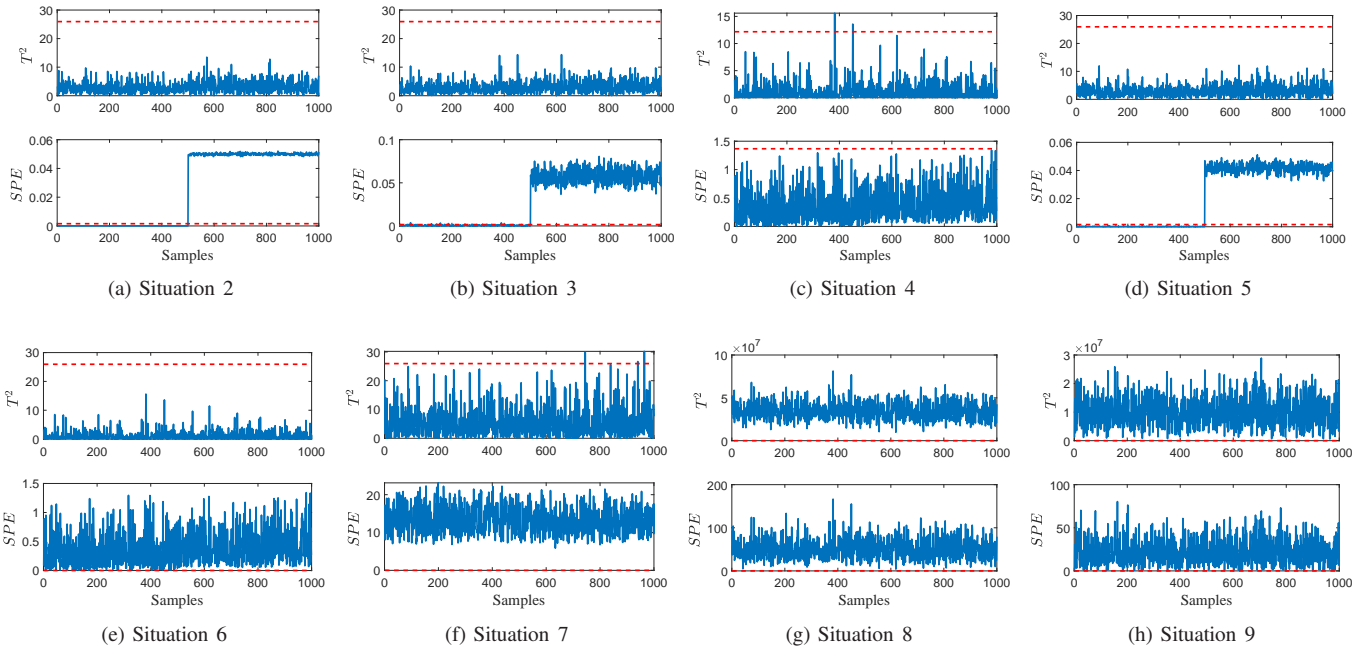


Fig. 2. Monitoring charts of Fault 1

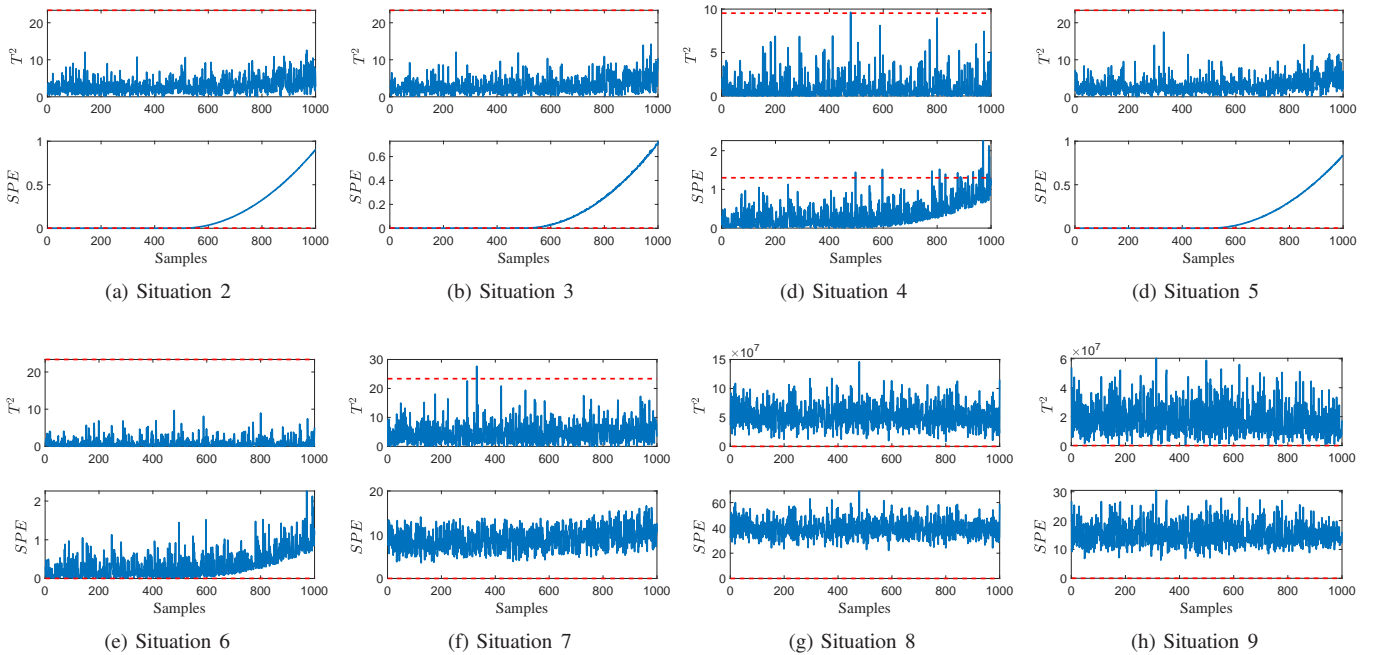


Fig. 3. Monitoring charts of Fault 3

TABLE II
EVALUATION INDEXES OF THE NUMERICAL CASE STUDY

Fault type	Fault 1			Fault 2			Fault 3		
Indexes	FDR(%)	FAR(%)	DD	FDR(%)	FAR(%)	DD	FDR(%)	FAR(%)	DD
Situation 1	100/0	$< 10^{-2}$	0/0	100/0	$< 10^{-2}$	0/0	98.82/0.14	0/0	5.82/0.7695
Situation 2	100/0	$< 10^{-2}$	0/0	100/0	$< 10^{-2}$	0/0	95.52/0.29	$< 10^{-2}$	5.82/0.7695
Situation 3	100/0	2.87/7.39	0/0	100/0	2.54/7.12	0/0	95.85/0.78	2.49/7.04	17.808/6.9590
Situation 4	0.15/0.09	1.01/1.63	0/0	0/0.14	$< 10^{-2}$	0/0	0.37/0.97	$< 10^{-2}$	17.808/6.9590
Situation 5	100/0	2.87/7.39	0/0	100/0	2.54/7.12	0/0	95.90/0.82	2.50/7.03	17.8152/6.9592
Situation 6	100/0	73.09/32.00	0/0	100/0	72.81/33.12	0/0	99.70/0.39	70.78/34.17	0.8610/1.6794
Situation 7	100/0	100/0	0/0	100/0	100/0	0/0	100/0	100/0	0/0
Situation 8	100/0	100/0	0/0	100/0	100/0	0/0	100/0	100/0	0/0
Situation 9	100/0	100/0	0/0	100/0	100/0	0/0	100/0	100/0	0/0

illustrate the effectiveness of PCA. As PCA is extremely popular, the monitoring charts of Situation 1 are no longer depicted owing to the space limitations.

Detailed explanations are described below. For Fault 1, the partial simulation results are illustrated in Fig. 2. The FDR of Situation 1 is 100% and it indicates that we get an accurate training model for the mode \mathcal{M}_1 . Outstanding performance is also reflected on Situation 2 in Fig. 2a, which implies that PCA-EWC is effective for monitoring the mode \mathcal{M}_2 . The Model B performs excellently on the mode \mathcal{M}_1 and the FDR of Situation 3 is 100%. It signifies that partial information of the mode \mathcal{M}_1 is retained when PCA is utilized for the current mode \mathcal{M}_2 , which is sufficient to provide optimal performance. Combining Situations 2 and 3, we discover that the Model B is effective for monitoring modes \mathcal{M}_1 and \mathcal{M}_2 simultaneously. However, the performance of Situation 4 is especially poor and the FDR approaches to 0. Comparing Situation 4 with Situation 3, the learned knowledge from the mode \mathcal{M}_1 has been forgotten visually and the performance decreases disastrously by PCA. The monitoring model by PCA in one mode fails to detect novelty in another mode. The result of Situation 5 in Fig. 2d is pretty excellent, which illustrates that PCA-EWC also provides optimal performance and continual learning ability for similar modes. For GMMs and RPCA, faults and normal data can not be distinguished in Figs. 2e-2h. As mentioned in the introduction section, the current methods for multimode process monitoring suffer from the “catastrophic forgetting” issue, as the simulation results of the comparative approaches illustrated. The analysis aforementioned is also applicable to Fault 2 and Fault 3 in Fig. 3. There exists detection delay for Fault 3 and the expected means are 5.82 or 17.8, which are acceptable because the fault amplitudes are 0.008 and 0.035, respectively.

According to the above-mentioned analysis, PCA-EWC can preserve significant information from the previous monitoring tasks when learning the new monitoring task, thus catastrophic forgetting of PCA is overcome for successive modes. Besides, the retained partial information is adequate to deliver optimal performance and thus PCA-EWC is capable of monitoring the same or similar modes. In brief, PCA-EWC can achieve

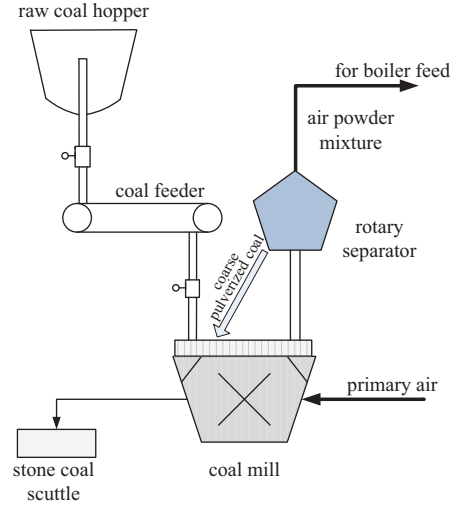


Fig. 4. Schematic diagram of the coal pulverizing system

favorable capability for monitoring multimode processes based on one model, without retraining from scratch.

B. Pulverizing system process monitoring

The 1000-MW ultra-supercritical thermal power plant is increasingly popular and highly complex. In this paper, we investigate one important unit of boiler, namely, the coal pulverizing system. The coal pulverizing system in Zhoushan Power Plant, Zhejiang Province, China, includes coal feeder, coal mill, rotary separator, raw coal hopper and stone coal scuttle, as shown in Fig. 4. It is expected to provide the proper pulverized coal with desired coal fineness and optimal temperature. The operating modes would vary owing to the types of coal and change of unit load.

We select the typical cases to illustrate the effectiveness of PCA-EWC, namely, abnormality from outlet temperature (Fault 4) and rotary separator (Fault 5). Detailed information is listed in Table III. The sample interval is 1 minute. Note that the number of training samples is abbreviated as NoTrS and the number of testing samples is short for NoTeS.

TABLE III
FAULT INFORMATION AND EXPERIMENTAL DATA OF THE PRACTICAL COAL PULVERIZING SYSTEM

Fault type	Key variables	Mode number	NoTrS/NoTeS	Fault location	Fault cause
Fault 4	Nine variables: outlet temperature, pressure of air powder mixture, primary air temperature, hot/cold primary air main pressure, etc.	\mathcal{M}_1	2160/2880	909	Internal deflagration owing to high outlet temperature
		\mathcal{M}_2	1080/1080	533	Hot primary air electric damper failure
		\mathcal{M}_3	0/1440	626	Air leakage at cold and hot primary air interface
Fault 5	Nine variables: rotary separator speed and current, bearing temperature, instantaneous coal feeding capacity of coal feeder, etc.	\mathcal{M}_1	2880/1080	806	Frequency conversion cabinet output short circuit alarm
		\mathcal{M}_2	720/720	352	High temperature of rotary separator bearing
		\mathcal{M}_3	0/2160	134	Large vibration

TABLE IV
FAULT DETECTION RESULTS OF THE COAL PULVERIZING SYSTEM

Fault type	Index	Situation 1	Situation 2	Situation 3	Situation 4	Situation 5	Situation 6	Situation 7	Situation 8
Fault 4	FDR (%)	99.95	99.45	98.40	100	99.45	89.98	100	100
	FAR (%)	3.19	0	0	91.04	0	66.35	100	100
	DD	1	3	0	-	3	-	-	-
Fault 5	FDR (%)	100	100	88.60	100	100	95.63	100	100
	FAR (%)	0	3.70	0	26.32	5.98	61.54	100	100
	DD	0	0	7	-	0	-	-	-

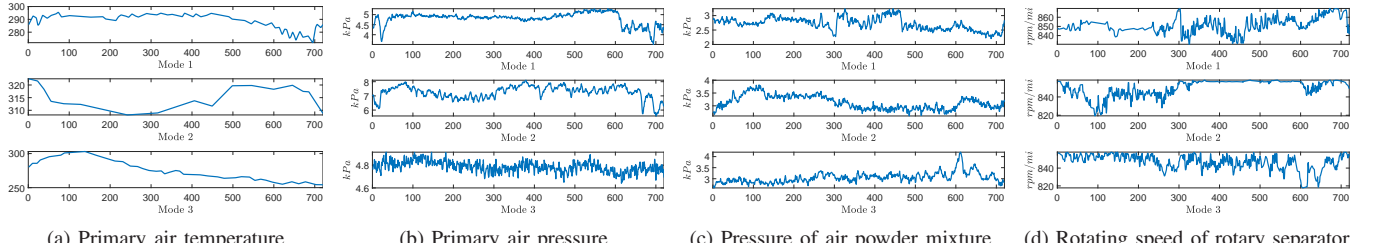


Fig. 5. Some variables of three modes: the first two figures are from normal data of Fault 4 and the last two are from normal data of Fault 5

The training data 1 and training data 2 come from modes \mathcal{M}_1 and \mathcal{M}_2 , respectively. Testing data i , are collected from mode \mathcal{M}_i , $i = 1, 2, 3$. Three modes occurred successively and have different mean values as well as standard deviations. Partial variables are exhibited in Fig. 5. We can find intuitively that data from three modes have a certain degree of similarity, especially the modes \mathcal{M}_1 and \mathcal{M}_3 . The similarity measured by Wasserstein distance also illustrates the above-mentioned result [42]. Some variables from different modes may have similar operating values. Four situations are designed according to Table I. As comparative experiments, four situations are designed below, which are a little different from the numerical case study.

- Situation 5: the GMMs-based monitoring model is built based on the normal data from modes \mathcal{M}_1 and \mathcal{M}_2 , the testing data are from mode \mathcal{M}_2 , which is utilized to illustrate the effectiveness on the trained mode;
- Situation 6: the training model is the same with Situation 5 and the testing data are from mode \mathcal{M}_3 to illustrate the effectiveness on similar mode;

- Situation 7: data contain the normal data from the mode \mathcal{M}_1 and the testing data from mode \mathcal{M}_2 to illustrate the effect of RPCA for monitoring the similar mode;
- Situation 8: data contain the normal data from modes \mathcal{M}_1 and \mathcal{M}_2 , testing data from mode \mathcal{M}_3 , which is employed to illustrate the effect of RPCA for monitoring the successive similar modes.

The monitoring charts of Fault 4 are presented in Fig. 6. PCA can detect the fault of the mode \mathcal{M}_1 and the FDR is 99.95%. The detection delay is 1 minute and acceptable. Then, PCA-EWC can also monitor the mode \mathcal{M}_2 accurately and the FAR is 0. Besides, the Model B performs well on the mode \mathcal{M}_3 and the FDR is 100%, as illustrated in Fig. 6c. It illustrates the continual learning ability of PCA-EWC for monitoring successive modes. In other words, after training the new mode based on PCA-EWC, we can still acquire excellent performance of the modes, which are similar to previous trained modes. In Fig. 6d, the FAR is more than 90% and the training Model C fails to detect the fault. It is meaningless to mention FDR and detection delay here. Furthermore, it verifies that PCA completely forgets the information of previous

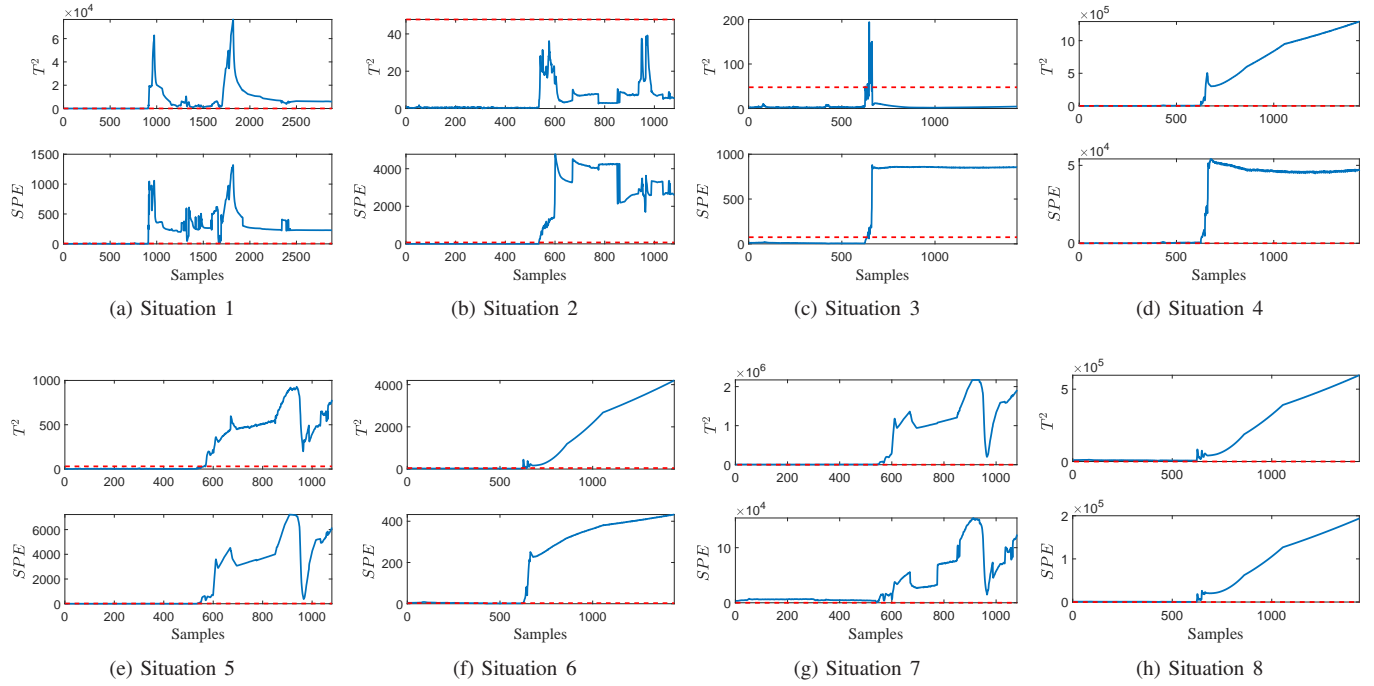


Fig. 6. Monitoring charts of Fault 4

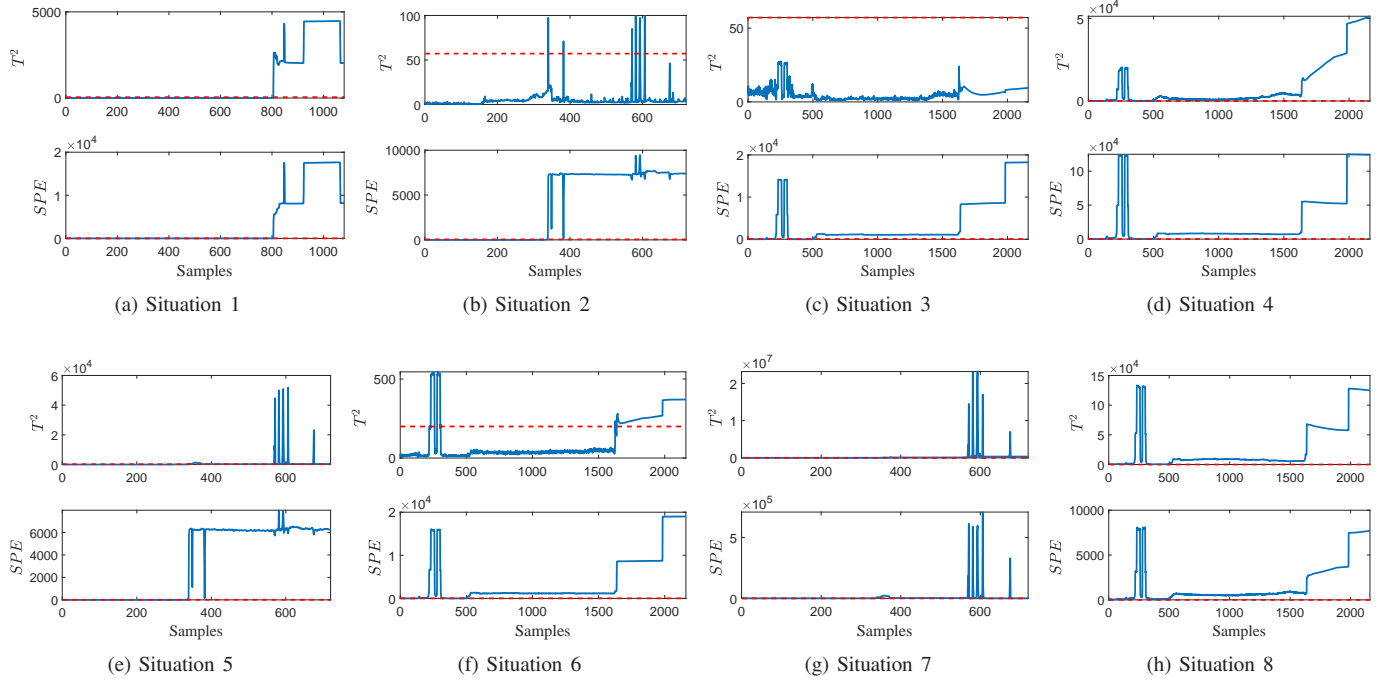


Fig. 7. Monitoring charts of Fault 5

modes and the previous learned knowledge is over-written by new information, thus leading to an abrupt performance decrease for monitoring previous modes. GMMs can provide excellent performance for the trained mode and the FDR is 99.45%, as illustrated in Fig. 6e. However, GMMs fail to monitor the similar mode that is not trained before and the FAR is 66.35% in Fig. 6f. In Figs. 6g and 6h, RPCA is not capable of tracking the successive modes and detecting faults accurately. The monitoring consequences of Fault 5 are shown in Fig. 7. The above-mentioned analysis of Fault 4 applies equally to Fault 5. Although the FAR of situation 4 is much lower than that of Fault 4, it is over 20% and not acceptable.

Take the data from Fault 4 as an example to highlight the superiorities of PCA-EWC further. To represent the immediate results intuitively, the first two components of projection vectors are shown in Fig. 8. The normal data from mode \mathcal{M}_3 are employed to train the PCA model. The cosine similarity measure is adopted to evaluate the similarity. Modes \mathcal{M}_1 and \mathcal{M}_3 have a certain degree of similarity while \mathcal{M}_2 and \mathcal{M}_3 are greatly different, as described in Fig. 8a. If the single monitoring model is established based on the traditional approaches, the features of mode \mathcal{M}_1 are over-written. When the mode \mathcal{M}_3 arrives, the current model based on data from mode \mathcal{M}_2 fails to provide the excellent performance. However, when PCA-EWC is adopted to preserve the significant features of mode \mathcal{M}_1 , the projection vector is similar to that of mode \mathcal{M}_3 in Fig. 8b, thus delivering the outstanding monitoring performance.

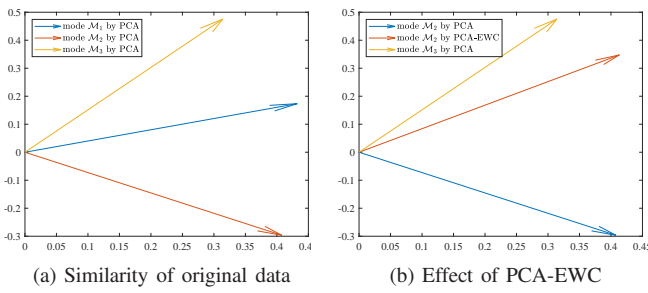


Fig. 8. Illustrations of superiorities of PCA-EWC

Besides, the actual computational time is considered in this paper. The sample interval is 1 minute. For Situations 1-4, the training time and the testing time are less than 0.1 second, which obviously satisfies the requirement of this practical industrial system. For GMMs, the monitoring model needs to be retrained when new modes occur and the time computational complexity would increase. The training complexity of GMMs is much higher than that of PCA-EWC and the testing complexity is similar. Besides, RPCA is more computationally complicated than PCA-EWC as the parameters are updated based on the new data for RPCA.

The simulation results are summarized in Table IV. According to the comparison among eight situations, PCA-EWC can preserve significant information of previous modes and it is enough to monitor the new similar modes precisely. However, traditional PCA forgets most information of previous monitoring tasks when a PCA-based model is built for the current

mode, and thus the performance is decreased catastrophically. GMMs and RPCA fail to monitor the successive modes and the monitoring mode needs to be retrained for GMMs.

VI. CONCLUSION

This paper provides a novel framework PCA-EWC with continual learning ability for monitoring multimode processes. The proposed algorithm adopts EWC to tackle the catastrophic forgetting of significant features of previous modes if PCA-based monitoring models are used, and the geometric illustration is depicted to understand the core thoroughly. The designed objective function of PCA-EWC is nonconvex and reformulated as DC programming, where the optimal solution is calculated thereafter. The spirit of PCA-EWC has been extended to more general multimode processes and the detailed implementing procedure has been presented. Moreover, the comparison between PCA and PCA-EWC is discussed from computational complexity. It has been interpreted that PCA-EWC is reformulated as PCA by specific parameter setting and slightly complicated than PCA. Besides, PCA-EWC preserves partial information of previous modes when modified PCA is utilized for the current mode. However, traditional PCA-based models can't remember the significant features of previous modes, and thus resulting in the abrupt decrease of performance if single local monitoring model is used. Compared with GMMs and RPCA, the effectiveness of PCA-EWC has been illustrated by a numerical case and a practical industrial system.

In future, we will resolve the problem that the number of principal components remains the same, multimode non-stationary process monitoring with continual learning ability would be investigated also. Besides, transfer learning will be considered to monitor the entirely different modes from previous ones.

APPENDIX

A. Details of Laplace approximation

Assume that model for mode \mathcal{M}_1 has been already built when data \mathbf{X}_2 are collected. The optimal parameter is

$$\theta_{\mathcal{M}_1}^* = \arg \min_{\theta} \{ -\log p(\theta | \mathbf{X}_1) \} \quad (36)$$

Obviously, $\partial \log p(\theta | \mathbf{X}_1) / \partial \theta = 0$ at $\theta_{\mathcal{M}_1}^*$. Based on the second order Taylor series around $\theta_{\mathcal{M}_1}^*$, $-\log p(\theta | \mathbf{X}_1)$ can be approximated as

$$-\log p(\theta | \mathbf{X}_1) \approx \frac{1}{2} (\theta - \theta_{\mathcal{M}_1}^*)^T \mathbf{H}(\theta_{\mathcal{M}_1}^*) (\theta - \theta_{\mathcal{M}_1}^*) + \text{constant} \quad (37)$$

where $\mathbf{H}(\theta_{\mathcal{M}_1}^*)$ is the Hessian matrix of $-\log p(\theta | \mathbf{X}_1)$ with respect to θ at $\theta_{\mathcal{M}_1}^*$. Since $\theta_{\mathcal{M}_1}^*$ is a local minimum, $\mathbf{H}(\theta_{\mathcal{M}_1}^*)$ is positive semi-definite and approximated by

$$\mathbf{H}(\theta_{\mathcal{M}_1}^*) \approx N_1 \mathbf{F}(\theta_{\mathcal{M}_1}^*) + \mathbf{H}_{\text{prior}}(\theta_{\mathcal{M}_1}^*) \quad (38)$$

where N_1 is the number of data \mathbf{X}_1 , $\mathbf{F}(\theta_{\mathcal{M}_1}^*)$ is the Fisher information matrix for mode \mathcal{M}_1 , $\mathbf{H}_{\text{prior}}$ is the Hessian matrix of $-\log p(\theta)$ and $\log p(\theta)$ is the prior of parameters. Here we assume that the prior is an isometric Gaussian prior,

and $\mathbf{H}_{prior}(\theta_{\mathcal{M}_1}^*) = \lambda_{prior} \mathbf{I}$ is adopted. According to (37-38), the Laplace approximation of (2) is reformulated as

$$\begin{aligned} \log p(\theta|\mathbf{X}) &\approx \log p(\mathbf{X}_2|\theta) - \frac{1}{2}(\theta - \theta_{\mathcal{M}_1}^*)^T \\ &\quad (N_1 \mathbf{F}_{\mathcal{M}_1} + \lambda_{prior} \mathbf{I})(\theta - \theta_{\mathcal{M}_1}^*) + \text{constant} \end{aligned} \quad (39)$$

B. Recursive Laplace approximation

Recursive Laplace approximation [36] is employed to approximate the objective function (26).

The posterior probability $\log p(\theta|\mathbf{X}_1, \mathbf{X}_2)$ is approximated by (3). Similar to Appendix A, Taylor series approximation is applied around $\theta_{\mathcal{M}_2}^*$ and the first order deviation is zero. The Hessian matrix of $-\log p(\mathbf{X}_2|\theta)$ can be approximated and replaced by $\lambda_{\mathcal{M}_2} \mathbf{F}_{\mathcal{M}_2}$, where $\mathbf{F}_{\mathcal{M}_2}$ is the Fisher information matrix of data \mathbf{X}_2 [36]. Besides, the second derivative of quadratic penalty is $\Omega_{\mathcal{M}_1}$. Thus, (26) is approximated as:

$$\begin{aligned} \log p(\theta|\mathbf{X}) &\approx \log p(\mathbf{X}_3|\theta) - (\theta - \theta_{\mathcal{M}_2}^*)^T \\ &\quad \Omega_{\mathcal{M}_2}(\theta - \theta_{\mathcal{M}_2}^*) + \text{constant} \end{aligned} \quad (40)$$

where

$$\Omega_{\mathcal{M}_2} = \Omega_{\mathcal{M}_1} + \frac{1}{2} \lambda_{\mathcal{M}_2} \mathbf{F}_{\mathcal{M}_2} \quad (41)$$

REFERENCES

- [1] T. J. Rato, J. Blue, J. Pinaton, and M. S. Reis, "Translation-invariant multiscale energy-based PCA for monitoring batch processes in semiconductor manufacturing," *IEEE Transactions on Automation Science and Engineering*, vol. 14, no. 2, pp. 894–904, 2017.
- [2] E. Skordilis and R. Moghaddass, "A double hybrid state-space model for real-time sensor-driven monitoring of deteriorating systems," *IEEE Transactions on Automation Science and Engineering*, vol. 17, no. 1, pp. 72–87, 2020.
- [3] N. Sheng, Q. Liu, S. J. Qin, and T. Chai, "Comprehensive monitoring of nonlinear processes based on concurrent kernel projection to latent structures," *IEEE Transactions on Automation Science and Engineering*, vol. 13, no. 2, pp. 1129–1137, 2016.
- [4] M. S. Tootooni, P. K. Rao, C. Chou, and Z. J. Kong, "A spectral graph theoretic approach for monitoring multivariate time series data from complex dynamical processes," *IEEE Transactions on Automation Science and Engineering*, vol. 15, no. 1, pp. 127–144, 2018.
- [5] O. F. Beyca, P. K. Rao, Z. Kong, S. T. S. Bukkapatnam, and R. Komanduri, "Heterogeneous sensor data fusion approach for real-time monitoring in ultraprecision machining (UPM) process using non-parametric Bayesian clustering and evidence theory," *IEEE Transactions on Automation Science and Engineering*, vol. 13, no. 2, pp. 1033–1044, 2016.
- [6] S. Yin, S. X. Ding, X. Xie, and H. Luo, "A review on basic data-driven approaches for industrial process monitoring," *IEEE Transactions on Industrial Electronics*, vol. 61, no. 11, pp. 6418–6428, 2014.
- [7] K. E. S. Pilario and C. Yi, "Canonical variate dissimilarity analysis for process incipient fault detection," *IEEE Transactions on Industrial Informatics*, vol. 14, no. 12, pp. 5308–5315, 2018.
- [8] K. Huang, Y. Wu, C. Yang, G. Peng, and W. Shen, "Structure dictionary learning-based multimode process monitoring and its application to aluminum electrolysis process," *IEEE Transactions on Automation Science and Engineering*, pp. 1–15, 2020.
- [9] W. Shao, Z. Ge, L. Yao, and Z. Song, "Bayesian nonlinear Gaussian mixture regression and its application to virtual sensing for multimode industrial processes," *IEEE Transactions on Automation Science and Engineering*, vol. 17, no. 2, pp. 871–885, 2020.
- [10] D. Zurita, M. Delgado, J. A. Carino, and J. A. Ortega, "Multimodal forecasting methodology applied to industrial process monitoring," *IEEE Transactions on Industrial Informatics*, vol. 14, no. 2, pp. 494–503, 2018.
- [11] J. Yu and S. J. Qin, "Multimode process monitoring with Bayesian inference-based finite Gaussian mixture models," *AIChE Journal*, vol. 54, no. 7, pp. 1811–1829, 2008.
- [12] W. Du, Y. Tian, and F. Qian, "Monitoring for nonlinear multiple modes process based on LL-SVDD-MRDA," *IEEE Transactions on Automation Science and Engineering*, vol. 11, no. 4, pp. 1133–1148, 2014.
- [13] Y. Q. Chen, O. Fink, and G. Sansavini, "Combined fault location and classification for power transmission lines fault diagnosis with integrated feature extraction," *IEEE Transactions on Industrial Electronics*, vol. 65, no. 1, pp. 561–570, 2018.
- [14] J. P. Liu, O. F. Beyca, P. K. Rao, Z. J. Kong, and S. T. S. Bukkapatnam, "Dirichlet process Gaussian mixture models for real-time monitoring and their application to chemical mechanical planarization," *IEEE Transactions on Automation Science and Engineering*, vol. 14, no. 1, pp. 208–221, 2017.
- [15] H. Ma, Y. Hu, and H. Shi, "A novel local neighborhood standardization strategy and its application in fault detection of multimode processes," *Chemometrics and Intelligent Laboratory Systems*, vol. 118, pp. 287–300, 2012.
- [16] X. Deng, N. Zhong, and L. Wang, "Nonlinear multimode industrial process fault detection using modified kernel principal component analysis," *IEEE Access*, vol. 5, pp. 23121–23132, 2017.
- [17] W. Li, H. H. Yue, S. Valle-Cervantes, and S. J. Qin, "Recursive PCA for adaptive process monitoring," *Journal of Process Control*, vol. 10, no. 5, pp. 471–486, 2000.
- [18] B. Wang, Z. Li, Z. Dai, N. Lawrence, and X. Yan, "Data-driven mode identification and unsupervised fault detection for nonlinear multimode processes," *IEEE Transactions on Industrial Informatics*, vol. 16, no. 6, pp. 3651–3661, 2020.
- [19] X. Xu, L. Xie, and S. Wang, "Multimode process monitoring with PCA mixture model," *Computers & Electrical Engineering*, vol. 40, no. 7, pp. 2101–2112, 2014.
- [20] X. Peng, Y. Tang, W. Du, and F. Qian, "Multimode process monitoring and fault detection: A sparse modeling and dictionary learning method," *IEEE Transactions on Industrial Electronics*, vol. 64, no. 6, pp. 4866–4875, 2017.
- [21] K. Peng, K. Zhang, B. You, and J. Dong, "Quality-related prediction and monitoring of multi-mode processes using multiple PLS with application to an industrial hot strip mill," *Neurocomputing*, vol. 168, pp. 1094–1103, 2015.
- [22] M. Quiñones-Grueiro, A. Prieto-Moreno, C. Verde, and O. Llanes-Santiago, "Data-driven monitoring of multimode continuous processes: A review," *Chemometrics and Intelligent Laboratory Systems*, vol. 189, pp. 56–71, 2019.
- [23] C. V. Nguyen, Y. Li, T. D. Bui, and R. E. Turner, "Variational continual learning," in *International Conference on Learning Representations 2018 (ICLR 2018)*, 2018.
- [24] P. Dhar, R. V. Singh, K.-C. Peng, Z. Wu, and R. Chellappa, "Learning without memorizing," in *2019 IEEE/CVF Conference on Computer Vision and Pattern Recognition (CVPR)*, pp. 5138–5146, 2019.
- [25] G. I. Parisi, R. Kemker, J. L. Part, C. Kanan, and S. Wermter, "Continual lifelong learning with neural networks: A review," *Neural Networks*, vol. 113, pp. 54–71, 2019.
- [26] P. R. Dachapally and M. N. Jones, "Catastrophic interference in neural embedding models," *Cognitive Science*, 2018.
- [27] R. Aljundi, *Continual Learning in Neural Networks*. PhD thesis, University of Oxford, 2019.
- [28] J. Kirkpatrick, R. Pascanu, N. Rabinowitz, J. Veness, G. Desjardins, A. A. Rusu, K. Milan, J. Quan, T. Ramalho, and A. Grabska-Barwinska, "Overcoming catastrophic forgetting in neural networks," *Proceedings of the National Academy of Sciences of the United States of America*, vol. 114, no. 13, pp. 3521–3526, 2017.
- [29] Z. Xiaojin, "An optimal D.C. decomposition algorithm for quadratic program with a single quadratic constraint," *OR Transactions*, vol. 013, no. 003, pp. 111–118, 2009.
- [30] Z. Li, J. Zhang, and Z. Wang, "Self-starting control chart for simultaneously monitoring process mean and variance," *International Journal of Production Research*, vol. 48, no. 15, pp. 4537–4553, 2010.
- [31] D. M. Hawkins and E. M. Maboudou-Tchao, "Self-starting multivariate exponentially weighted moving average control charting," *Technometrics*, vol. 49, no. 2, pp. 199–209, 2007.
- [32] Y. Li, Y. Liu, C. Zou, and W. Jiang, "A self-starting control chart for high-dimensional short-run processes," *International Journal of Production Research*, vol. 52, no. 1–2, pp. 445–461, 2014.
- [33] G. Capizzi and G. Masarotto, "Self-starting CUSCORE control charts for individual multivariate observations," *Journal of Quality Technology*, vol. 42, no. 2, pp. 136–151, 2010.
- [34] H. J. Sussmann, "Uniqueness of the weights for minimal feedforward nets with a given input-output map," *Neural Networks*, vol. 5, no. 4, pp. 589–593, 1992.

- [35] MacKay and D. J. C, "A practical Bayesian framework for backpropagation networks," *Advances in Neural Information Processing Systems*, vol. 4, no. 3, pp. 448–472, 1992.
- [36] F. Huszár, "On quadratic penalties in elastic weight consolidation," *arXiv preprint arXiv:1712.03847*, 2017.
- [37] J. C. O. Souza, P. R. Oliveira, and A. Soubeyran, "Global convergence of a proximal linearized algorithm for difference of convex functions," *Optimization Letters*, vol. 10, no. 7, pp. 1–11, 2015.
- [38] B. Nguyen and B. De Baets, "An approach to supervised distance metric learning based on difference of convex functions programming," *Pattern Recognition*, vol. 81, pp. 562–574, 2018.
- [39] J. Huang, F. Nie, H. Huang, and C. Ding, "Robust manifold nonnegative matrix factorization," *ACM Transactions on Knowledge Discovery from Data (TKDD)*, vol. 8, no. 3, pp. 1–21, 2014.
- [40] J. Zhang, H. Chen, S. Chen, and X. Hong, "An improved mixture of probabilistic PCA for nonlinear data-driven process monitoring," *IEEE Transactions on Cybernetics*, vol. 49, no. 1, pp. 198–210, 2019.
- [41] C. Tong and X. Yan, "A novel decentralized process monitoring scheme using a modified multiblock PCA algorithm," *IEEE Transactions on Automation Science and Engineering*, vol. 14, no. 2, pp. 1129–1138, 2017.
- [42] J. A. Carrillo and G. Toscani, "Wasserstein metric and large-time asymptotics of nonlinear diffusion equations," in *Proceedings of the International Meeting*, pp. 234–244, 2005.